Hard X-ray Resonant Ptychography for Chemical Imaging at the Sensitivity Limit.

Juliane Reinhardt[1,2*], Andreas Schropp[3], Mikhail Lyubomirskiy[3], Martin Seyrich[3], Dennis Brückner[3], Thomas F. Keller[3,4], Vedran Vonk[3], Sergey Volko[3], Andreas Stierle[3,4], Edvinas Navickas[5], Jürgen. Fleig[5] and Christian G. Schroer[3,4]

[1] Australian Synchrotron and La Trobe University, Dept. of Chemistry and Physics, Melbourne, Australia
[2] Australian Research Council, Centre of Excellence for Advanced Molecular Imaging, Australia
[3] Deutsches Elektronen-Synchrotron, Hamburg, Germany
[4] University of Hamburg, Department Physik, Hamburg, Germany
[5] Technical University Wien, Institute for Chemical Technologies and Analytics, Vienna, Austria
* Corresponding author: juliane.reinhardt@synchrotron.org.au

The imaging technique ptychography is based on scattering of coherent light, in the present case of coherent X-rays, and allows for the reconstruction of the complex-valued object transmission function, which is a measure of the attenuation and the phase shift that the X-rays undergo while transmitting through the object. Since the spatial resolution in a reconstructed image depends on the highest scattering angle, at which a signal can still be detected over noise and over background scattering, ptychography overcomes the resolution limit given by X-ray optics [1]. The interaction of X-rays with matter is energy-dependent and strongly varying for photon energies close to the binding energies of electrons in the atom (resonance). Consequently, as the scattering contrast changes differently at distinct energies for different materials, resonant ptychography is sensitive to the elemental and chemical distribution of the sample [2]. The evaluation of resonant datasets for nanoanalysis demands high quality of the individual ptychographic reconstructions in terms of spatial resolution, sensitivity, stability and positioning accuracy. Here, we present two examples of our latest efforts in advancing hard X-ray resonant ptychography for high-sensitivity imaging in combination with elemental and chemical contrast [5].

We investigated a catalyst model specimen containing gold, platinum and palladium nanoparticles ranging from $10\,\mathrm{nm}$ to $100\,\mathrm{nm}$ in diameter. We achieved a high reconstruction quality by applying a double exposure scheme using an opaque beamstop to significantly suppress parasitic background [3] and by adding further constraints to the reconstruction algorithm [4]. Based on ptychographic reconstructions at different energies, we extracted the elemental distribution with a phase shift sensitivity of $\pm 5\,\mathrm{mrad}$ and a spatial resolution better than $15\,\mathrm{nm}$ [3]. The 2D map in Fig. 1a shows the difference between two phase shift reconstructions – one at the photon energy of $11.918\,\mathrm{keV}$ at the Au-L$_3$ edge and one at $11.55\,\mathrm{keV}$ close to the Pt-L$_3$ edge. The expected phase shift difference, calculated from EXAFS reference measurements, for gold between these two energies is about $-20\,\mathrm{mrad}$ and about $+15\,\mathrm{mrad}$ for platinum. The 2D difference map agrees well with the phase shift estimation and also matches the elemental distribution obtained from the energy-dispersive X-ray spectroscopy SEM image shown in Fig. 1b.

We have also investigated oxidation states in a platinum layer on yttria-stabilised zirconia (Pt(O$_2$)/YSZ). This system is one of the most prominent solid state electrode systems used in chemical sensors or solid oxide fuel cells. During electrochemical treatment, the platinum layer forms bubbles, which are suspected to contain different oxidation states of platinum and play a key role in understanding the degradation of these devices. For this experiment we performed a 2D ptychographic scan at 46 energies around the Pt-L$_3$ edge. In the resulting energy stack of phase shift reconstructions, the phase shift value $\phi(E)$ in each

pixel exhibits a discrete spectrum of a mixture of metallic and oxidised platinum. Such a mixture of different oxidation states in bulk material can be described by the superposition of all these different states weighted by their proportion. In order to find this composition, phase shift references for metallic platinum $A(E)$ and oxidised platinum $B(E)$ were fitted to the phase shift values $\phi(E)$ from the ptchographic reconstruction by minimising the cost function F:

$$F = \sum_E \left[\phi(E) - (d_A \cdot A(E) + d_A \cdot B(E) + \phi_{\mathrm{const}})\right]^2 \ \to \min$$

where $A(E) = \frac{2\pi}{\lambda} \cdot \delta_A(E)$ and $B(E)$ defined analogously, with λ the wavelength corresponding to the photon energy E and δ the refractive index. The optimisation parameters d_A, d_B represent the effective thickness of the metallic and oxidised state, respectively, and ϕ_{const} covers a non-resonant phase shift offset caused by other materials in the sample volume. With the optimised output for d_A, d_B and ϕ_{const}, the total effective thickness d of the sample along the projection direction as well as the percentages for the metallic and oxidised state were calculated. To illustrate the Pt bubble, Fig. 1e shows an SEM image of a generic Pt bubble sliced using FIB and a single ptychographic phase reconstruction in Fig. 1c. The result for the percentage of oxidised platinum in the Pt bubble along the projection direction in each pixel as a result of the fitting routing is visualised in the 2D image in Fig. 1d. Although connected areas of higher concentration of oxidised material are present in this 2D image, high residuals (not shown here) of the individual fitting curves indicate deviations of the phase shift values from the model. Detailed analysis identified drifts and positioning errors as well as a high amount of carbon contamination accumulated during the measurement as error sources. Consequently, the final determination of the chemical distribution must be discussed carefully and is only valid for higher amounts of oxidised platinum in thicker areas.

In conclusion, we demonstrated that resonant ptychography provides access to the elemental and chemical distribution of different kinds of samples. We explored the sensitivity limits arising from experimental restrictions such as background scattering, position accuracy and carbon deposit that can be circumvented in future experiments by controlling the sample environment. Hard X-ray resonant ptychography, also in combination with tomography, has the potential for many different applications where high spatial resolution is required to determine the chemical distribution in bulk material.

References:

[1] A. Schropp et al., Appl. Phys. Lett. **100**, 253112 (2012)
[2] R. Hoppe, J. Reinhardt et al., Appl. Phys. Lett. **102**, 203104 (2013)
[3] J. Reinhardt et al., Ultramicroscopy **173**, 52-57 (2017)
[4] J. Reinhardt and C.G. Schroer, JINST, (2018, accepted)
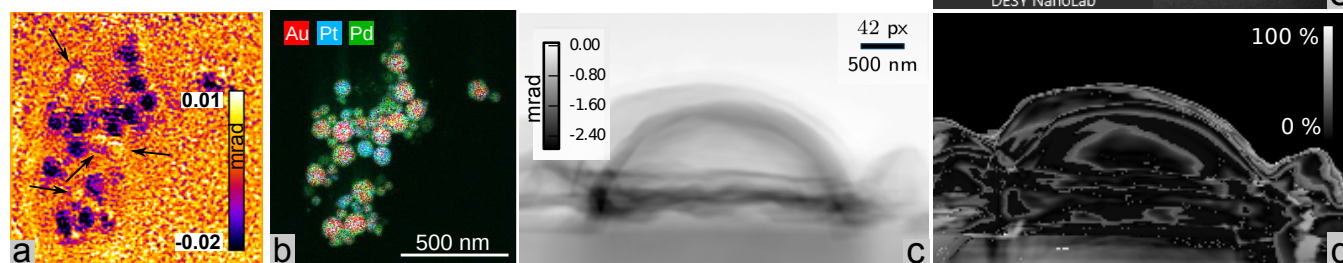[5] J. Reinhardt, PhD thesis (2017)

Figure 1: (a) Difference in the phase shift reconstruction between the Au-L_3 and Pt-L_3 edges revealing the elemental distribution, dark spheres depict gold and bright spheres platinum (arrows). It agrees with the elemental distribution obtained from EDX SEM measurements in (b). (c) shows the phase reconstruction of the Pt bubble and (d) shows a 2D distribution of oxidised platinum in the Pt bubble in percent. (e) shows an SEM image of a generic Pt bubble.